Atmos. Chem. Phys. Discuss., 9, 16267–16294, 2009
www.atmos-chem-phys-discuss.net/9/16267/2009/


Atmospheric Chemistry and Physics Discussions

This discussion paper is/has been under review for the journal *Atmospheric Chemistry and Physics (ACP)*. Please refer to the corresponding final paper in *ACP* if available.

# Constraining the concentration of the hydroxyl radical in a stratocumulus-topped marine boundary layer from sea-to-air eddy covariance flux measurements of dimethylsulfide

**M. Yang, B. W. Blomquist, and B. J. Huebert**

Department of Oceanography, University of Hawaii, Honolulu, HI, USA

Received: 20 July 2009 – Accepted: 23 July 2009 – Published: 30 July 2009

Correspondence to: B. J. Huebert (huebert@hawaii.edu)

Published by Copernicus Publications on behalf of the European Geosciences Union.





## Abstract

The hydroxyl radical (OH) is an important oxidant in the troposphere due to its high reactivity and relative abundance. Measuring the concentration of OH in situ, however, is technically challenging. Here we present a robust yet simple method of estimating an OH-equivalent oxidant concentration ("effective OH") in the marine boundary layer (MBL) from the mass balance of dimethylsulfide (DMS). We use shipboard eddy covariance measurements of the sea-to-air DMS flux from the Vamos Ocean-Cloud-Atmosphere-Land Study Regional Experiment (VOCALS-REx) in October and November of 2008. The persistent stratocumulus cloud-cover off the west coast of South America and the associated strong inversion between MBL and the free troposphere (FT) greatly simplify the dynamics in this region and make our budget estimate possible. From the observed diurnal cycle in DMS concentration, the nighttime entrainment velocity at the inversion is estimated to be 4 mm $s^{-1}$. We calculate $1.4\times10^6$ OH molecules $cm^{-3}$ from the DMS budget, which represents a ~monthly effective OH concentration and is well within the range of previous estimates. Furthermore, when fitted to the measured intensity of solar flux, the resultant diel variation in OH concentration, together with the DMS surface and entrainment fluxes, enables us to accurately replicate the observed diurnal cycle in DMS (correlation coefficient exceeding 0.9). The nitrate radical is found to have little contribution to DMS oxidation during VOCALS-REx.

## 1 Introduction

While non-reactive towards the major constituents of the atmosphere, the hydroxyl radical (OH) is the principal oxidizing free radical in the troposphere for trace species (Levy, 1971). The primary source of OH is the reaction between water vapor and excited atomic oxygen ($O(^1D)$); the latter is a product of the photo-dissociation of ozone ($O_3$) by photons between 290 and 320 nm. Reduction of the hydroperoxy radical by ni-



ACPD

9, 16267–16294, 2009



trogen oxide (NO) also contributes to the production of OH (Donahue and Prinn, 1990). OH reacts readily with most trace gases and is often regenerated during the process, resulting in sustained OH concentrations on the order of $10^6$ molecules $cm^{-3}$ globally (Prinn et al., 1995; Spivakowsky et al., 2000). The radical is consumed primarily by reacting with carbon monoxide (CO), but it also reacts with sulfur dioxide ($SO_2$), nitrogen dioxide ($NO_2$), and a wide range of hydrocarbons. Models predict higher OH concentrations for the tropics and for the southern hemisphere. The former is attributed to higher humidity and solar fluxes that promote $O_3$ dissociation; the latter is presumably due to less CO south of the equator (a result of lower anthropogenic emissions; Seinfeld and Pandis, 2006).

Due to the transient nature of the radical, measuring OH in situ was not possible until the last two decades, when specialized instruments based on absorption, fluorescence, and mass spectroscopy were developed (e.g. Mount, 1992; Hard et al., 1984; Eisele and Tanner, 1991). However, direct observations of this radical cannot be made in all field experiments (such as during VOCALS-REx). Even when in situ OH measurements are available, they might not represent a temporal or regional average, which is of importance to large-scale models.

Alternatively, global and regional distributions of OH are often estimated by measuring chemicals with known lifetimes that are exclusively consumed by this radical, such as methyl chloroform (Prinn et al., 1992). Here we follow a similar approach and use a budget analysis of naturally-derived atmospheric dimethylsulfide (DMS) to constrain the equivalent OH concentration in a clean, stratocumulus-capped marine boundary layer.

Dimethylsulfide ($CH_3SCH_3$) in the open ocean ($DMS_w$) is derived exclusively from phytoplankton. Due to photochemical destruction and rapid dilution, the atmospheric concentration of DMS is always orders of magnitude lower than the expected Henry's law equilibrium concentration with $DMS_w$. Consequently, DMS gas always effluxes from the surface ocean and is the largest source of reduced sulfur to the atmosphere (Lovelock et al., 1972). The substantial magnitude of the flux and the lack of other



ACPD
9, 16267–16294, 2009



sources make DMS an ideal gas with which to study air-sea exchange. In the atmosphere, DMS is principally oxidized by OH to form sulfur dioxide, dimethylsulfoxide (DMSO) and methane sulfonic acid (MSA). $SO_2$ may be oxidized further to form sulfate, which contributes to aerosol growth and formation of cloud condensation nuclei (CCN). The coverage and lifetime of marine clouds formed from these CCN affect the earth's radiative balance and may in turn be linked to biological production in the ocean (Charlson et al., 1987).

The oxidation of DMS by OH proceeds through two separate pathways: the hydrogen-atom abstraction at a methyl group that subsequently leads to mostly $SO_2$:

$$CH_3SCH_3 + OH\cdot \xrightarrow{k1} CH_3SCH_2\cdot + H_2O \quad (1)$$

and the OH addition to the sulfur atom that can lead to a wider range of products, including DMSO and MSA:

$$CH_3SCH_3 + OH\cdot \xrightarrow{k2} CH_3\dot{S}(OH)CH_3 \quad (2)$$

The abstraction pathway is favored under high temperatures; the Arrhenius form for this rate constant is $k_1 = 1.1\times10^{-11}\exp(-240/T)$, equating to $4.9\times10^{-12}$ cm$^3$ molec$^{-1}$ s$^{-1}$ at 298 K. The addition pathway is favored under low temperatures; this oxygen ($O_2$) and temperature dependent rate constant is best represented by $k_2 = 1.0\times10^{-39}$ [$O_2$] $\exp(5820/T)/\{1+5.0\times10^{-30}$ [$O_2$]$\exp(6280/T)\}$ (Sander et al., 2006). At 298 K, about 80% of the oxidation of DMS goes through the abstraction pathway; this fraction lowers to half at 285 K (Stickel et al., 1993; Wallington et al., 1993).

Other oxidants, including nitrate and halogen radicals, may react with DMS as well. The nitrate radical ($NO_3$) is produced from the reaction between $NO_2$ and $O_3$, with $NO_2$ being one of the nitrogen oxides ($NO_x$). The DMS-$NO_3$ reaction proceeds through the hydrogen abstraction pathway. The Arrhenius form of this rate constant is $k_{NO_3} = 1.9\times10^{-13}\exp(500/T)$, equating to $1.0\times10^{-12}$ cm$^3$ molec$^{-1}$ s$^{-1}$ at 298 K (Sander et al., 2006), which is several times lower than that of the DMS-OH reaction. In contrast to OH, $NO_3$ can only have an appreciable concentration at night because it is



ACPD
9, 16267–16294, 2009



photolyzed rapidly during the day. Studies from Equatorial Christmas Island showed that in the remote Pacific, the contribution to DMS loss from $NO_3$ is less than a few percent due to the low levels of $NO_x$ away from anthropogenic activities (Davis et al., 1999; Chen et al., 2000). The same studies also suggested that the DMS-chorine reaction, while still very poorly understood, accounts for no more than 5~10% to the oxidation of DMS.

The aforementioned Christmas Island experiments have demonstrated a clear diurnal cycle of DMS in the MBL (Bandy et al., 1996; Davis et al., 1999). While the supply of DMS to the boundary layer via air-sea exchange is continuous, destruction of DMS principally takes place during the sunlit hours, when OH is available. As a result, DMS starts to increase from its daily minimum just before sunset and builds up through the night until just after sunrise, at which time photolysis causes DMS to decrease until near the next sunset. This diurnal cycle in DMS would be altered in a pollution-influenced marine environment where anthropogenically produced $NO_x$ level is high, as nighttime oxidation of DMS by $NO_3$ can be comparable in magnitude to daytime oxidation by OH (Yvon et al., 1996).

The equivalent OH we estimate here from VOCALS-REx is an effective concentration, the concentration of OH that would cause the same rate of DMS loss as if OH were the only oxidant. In all likelihood, our effective OH is slightly higher than the actual OH concentration, since it includes the minor contributions (mentioned above) from the other oxidants.

The VOCALS-REx experiment took place in October and November of 2008 in the Southeast Pacific, off the west coast of Chile and Peru (http://www.eol.ucar.edu/projects/vocals/). The experiment aimed to address the interactions among the ocean, atmosphere, and land in this tightly coupled regional climate system. The Andes mountain range to the east forces strong winds parallel to the coast. Ekman transport results in coastal upwelling of cold, nutrient-rich waters, which leads to stability in the lower troposphere. The warm, dry air over the cool water surface, together with the large-scale subsidence from the Hadley Cell, creates a widespread and persistent stratocumulus



ACPD
9, 16267–16294, 2009



cloud deck (Bretherton et al., 2004). These thin, low-lying, and hence radiatively-cooling clouds form from CCN aerosols. While anthropogenic aerosols dominate the coastal region, a significant fraction of CCN is likely derived from DMS-derived sulfate in the clean marine environment offshore (Charlson et al., 1987). From time to time, hundred-kilometer sized openings (which can be observed from satellites) form in the stratocumulus cloud-deck and advect with the mean wind. These features have been coined "pockets of open cells" (POCs) and are hypothesized to be related to drizzle removing CCN from the air (Stevens et al., 2003). To really understand this phenomenon then, we need to look at the origin and fate of the CCN-precursors, such as DMS and its oxidants.

A stratus/stratocumulus marine boundary layer is characterized by vigorous mixing due to the intense longwave radiative cooling at the cloud-top (Lilly, 1968). Air entrains down from the FT, which is balanced by a deepening of the MBL and wind divergence. The strong inversion in effect caps the MBL, confining surface-borne scalars like DMS. Therefore, stratocumulus regions such as the Southeast Pacific can be viewed as natural analogs to box models, with straightforward inputs and outputs. Our OH estimate was made possible as a result of these simplified conditions.

## 2 Experimental and methods

The National Oceanographic and Atmospheric Administration (NOAA) ship *Ronald H. Brown (RHB)* was deployed in the Southeast Pacific from approximately 24 October to 30 November 2008. In addition to retrieving and maintaining the Woods Hole Oceanographic Institute's Stratus buoy at 85° W and 20° S, a number of zonal transects were made at latitudes between 18.5° S and 21.5° S to survey eddies and upwelling features. The edges of such eddies are often associated with higher levels of biological productivity, hence more $DMS_w$ (T. Bates, P. Matrai, unpublished data). In the same general time frame, multiple aircraft, including the National Science Foundation (NSF)/National Center for Atmospheric Research (NCAR) C-130, repeatedly flew west-



ACPD
9, 16267–16294, 2009



ward from its base station in Arica, Chile to the stratocumulus region offshore. Most of the research flights were designed to survey the 20° S cross-section and study the formation and development of POCs.

During the experiment, two nearly identical atmospheric pressure ionization mass spectrometers (APIMS) were used to measure DMS on board of *RHB* and the C-130, the largest difference being that the instrument at sea was sampling at a high rate of 20 hz to quantify the sea-to-air flux, whereas the one aloft was measuring concentration every 10 s. The measurement of DMS by the APIMS with isotopically labeled standard technique has been described previously (Bandy et al., 2002; Huebert et al., 2004; Blomquist et al., 2006).

We estimate the OH-equivalent oxidant concentration from the budget analysis of DMS in the MBL. The conservation equation for any chemical species, $S$, in the marine boundary layer is represented in Eq. (3) (with the overbar representing a time-average):

$$\frac{\partial \overline{S}}{\partial t} + \overline{u}\frac{\partial \overline{S}}{\partial x} + \frac{\partial \overline{S'w'}}{\partial z} = P - L \tag{3}$$

The first term on the left represents the time-rate of change in the concentration of $S$. The second term is the horizontal advection of $S$ due to gradients along the mean wind ($u$). The third term is the flux divergence, the difference between vertical fluxes at the bottom and top of the box model. Local (chemical) production and loss of $S$ are represented by $P$ and $L$, respectively, on the right side of the conservation equation.

As described in the previous section, DMS fluxes upwards from the surface ocean to the stratocumulus-topped MBL, in which it is oxidized (principally by OH), diluted by DMS-free air entrained from the FT, and transported horizontally. DMS is not produced chemically, so $P$=0. Therefore the chemical loss due to oxidation can be calculated by closure if we know the DMS surface flux, entrainment flux, horizontal advection, and the time-rate of change in column concentration.

### 2.1 Surface flux of DMS

On the ship, the inlet of our mass spectrometer was located at 18 m above the water surface on the jackstaff, where flow-distortion due to the ship's superstructure is minimized. A precisely known amount of the triply-deuterated DMS standard was continuously injected at the inlet and combined with a high ambient air flow. The DMS concentration was determined from the ratio between the ambient and standard DMS mass spectrometer signals. Relative wind speeds, acceleration, and rotation in three axes were recorded at the same frequency as the DMS by a Gill Sonic anemometer and a Systron-Donner Motionpak accelerometer, respectively. Ship's motion was removed from relative winds to get true winds following Edson et al., (1998). To obtain surface flux ($F_0$) via eddy covariance, DMS concentration was correlated with the vertical wind velocity ($w$) in the form of $F_0 = \overline{\mathrm{DMS}' w'}$ (primes here denote deviations from the means). Flux was initially computed in ten-minute segments that overlapped by 50%. To remove times when sampling conditions were unfavorable, any ten-minute segment with relative wind direction more than 90 degrees off the bow or gyro heading changing by over 30 degrees (ship maneuvering) was screened out. The remaining "good" segments were averaged to hourly values.

Time-series of DMS concentration and surface flux from the *RHB* are shown in Fig. 1, with VOCALS averages of 57 pptv and 3.4 $\mu$moles $\mathrm{m}^{-2}\,\mathrm{day}^{-1}$, respectively. We limit our averaging to offshore observations only (73° W~86° W and 18° S~22° S, hereinafter "the VOCALS region"). Near-shore data were not included in the project average due to heterogeneities in the atmospheric DMS field caused by spikes in seawater DMS on the edges of localized, episodic coastal eddies.

Even with the ship steaming at up to 12 knots, the classic sinusoidal diurnal cycle in DMS was seen clearly on a number of days (Fig. 2). This observation implies a widespread homogeneity over the region with limited meso-scale variability. Continental influence, which is usually associated with high levels of $NO_x$, and thus high $NO_3$, should also be minimal.



ACPD
9, 16267–16294, 2009



## 2.2 Boundary layer structure

We use DMS concentration measured from the C-130 to infer the boundary layer structure and exchange between the MBL and FT. Figure 3 shows a typical profile of the lower troposphere during VOCALS-REx. The DMS concentration decreased gradually with altitude within the MBL and rapidly dropped to near-zero in the FT immediately above the stratocumulus cloud-top (as evidenced by the enhanced liquid water content). Dew point and potential temperature also showed sharp gradients at the same altitude.

To determine the inversion height, we looked for such sharp gradients in dew point and potential temperature in profiles from the C-130 profiles. Across a thin layer of a few tens of meters, the changes in dew point and potential temperature were of the order of 20 and 10 K, respectively. The boundary layer was deeper offshore (~1.5 km at 85° W) than at the coast (~1 km), as is typical of this region. The inversion heights determined from the aircraft agree very well with shipboard observations of cloud top from a W-band radar (24 m range gate, 50 m pulse length). On average, the stratocumulus cloud top varied from ~1350 m near dawn to ~1200 m near dusk (S. de Szoeke, personal communication, 2009).

When the MBL is shallow and well mixed, scalars with long lifetimes should be homogeneously distributed with altitude. Since DMS in the MBL came from the ocean surface and is diluted by entrainment above, we expect it to exhibit a decreasing concentration with height. Because its mixing time within the MBL (~1 h) is shorter than its lifetime (1~2 days, calculated later), the vertical gradient of DMS within the MBL is usually only a few pptv (Faloona et al., 2005). With an average inversion height of 1.3 km in the VOCALS region, this vertical gradient increased significantly with boundary layer depth. Figure 4 shows the averaged profile from the C-130 during the experiment. Altitude was normalized to the inversion height ($z_i$). DMS concentration aloft was normalized by its concentration at the lowest level ($DMS/DMS_0$). On average DMS immediately below the inversion was ~80% of what was at the surface, and the verti-



ACPD
9, 16267–16294, 2009



cal gradient appeared to be linear. $DMS/DMS_0$ was linearly regressed against $z/z_i$ in the MBL ($r^2$=0.8). The fraction of DMS relative to surface concentration can thus be parameterized as $1-\alpha(z/z_i)$, where $\alpha$ represents the "decoupling" parameter of DMS and is 0.2 on average. This formulation of the MBL structure is similar to what is used in Wood and Bretherton (2004).

### 2.3 Advective flux of DMS

During VOCALS, winds almost always came from the South/Southeast (150°). Despite local patchiness, DMS concentration and flux showed increasing trends away from the coast due to generally lower wind speeds near shore (Fig. 5). The ratio between the flux and concentration, however, was nearly constant with longitude. Also plotted is the inversion height estimated from C-130 profiles within the latitude range of 20±2° S.

We estimate the advective flux of DMS from horizontal gradients computed from shipboard DMS measurements. Using multi-variate linear regression, DMS in the VOCALS regions and to the east was regressed against latitude and longitude. Because the ship was sampling 24 h a day, we expect temporal biases (e.g. from the diel variability) to be small; time is thus omitted from the regression analysis. The fitting coefficients are found to be $-2\,\mathrm{pptv}\,^\circ\mathrm{Lon}^{-1}$ and $-1\,\mathrm{pptv}\,^\circ\mathrm{Lat}^{-1}$, with higher DMS towards the Southwest. MBL DMS measured from the C-130 shows a similar pattern. For an average wind speed of $6\,\mathrm{m\,s}^{-1}$ from 150°, multiplying the zonal and merdional winds ($-3$ and $5\,\mathrm{m\,s}^{-1}$, respectively) by the DMS gradient leads to an advective term (Eq. 3) of $0.04\,\mathrm{pptv\,h}^{-1}$. Integrating over the 1.3 km column gives an advective flux of only $0.05\,\mu\mathrm{moles\,m}^{-2}\,\mathrm{day}^{-1}$, less than 1% of the DMS sea-to-air flux. The low advective flux term was due to the fact that the mean wind direction was largely orthogonal to the horizontal DMS gradient; we will therefore set it to zero.



ACPD
9, 16267–16294, 2009



### 2.4 Entrainment velocity

To calculate the entrainment flux of DMS, we need to know the entrainment velocity at the inversion ($\omega_e$). While $\omega_e$ was not directly measured during VOCALS-REx, we can estimate it from the observed nighttime increase in DMS concentration. To remove the effect of changing MBL depth on the diurnal cycle in DMS concentration, we integrate the DMS concentration to the MBL height following the vertical gradient determined from Sect. 2.2, leading to column concentration is in units of $\mu$moles m$^{-2}$.

The integral form of Eq. (3) from the surface to the inversion height ($z_i$) is shown in Eq. (4), with the advection and production terms now dropped out. The angular brackets denote column integrals, with every term now in units of flux:

$$\frac{\partial \left\langle \overline{\mathrm{DMS}} \right\rangle}{\partial t} = F_0 - \omega_e\{[\mathrm{DMS}_{z_i^-}] - [\mathrm{DMS}_{z_i^+}]\} - k_{\mathrm{PFO}} \left\langle \overline{\mathrm{DMS}} \right\rangle \quad (4)$$

The term on the left side of Eq. (4) is the time-rate of change in column concentration. We have separated the flux divergence into the first and second terms on the right side of Eq. (4), representing the DMS fluxes at the ocean surface and inversion, respectively. The entrainment flux is formulated as the entrainment velocity, $\omega_e$, multiplied by the concentration jump across the inversion (Lilly, 1968), with $z_i^-$ and $z_i^+$ meaning just below and above $z_i$. The last term on the right represents the chemical loss of DMS, which has been expanded to be the product of $k_{\mathrm{PFO}}$ (a pseudo first order reaction rate constant) and DMS column concentration. We can parameterize the DMS concentration just below $z_i$ to be a fraction of the surface value ([DMS$_0$]) using the DMS "decoupling" parameter, $\alpha$. Since DMS above the inversion, in the FT was practically zero, Eq. 4 simplifies to:

$$\frac{\partial \left\langle \overline{\mathrm{DMS}} \right\rangle}{\partial t} = F_0 - \omega_e(1-\alpha)[\mathrm{DMS}_0]_i - k_{PFO} \left\langle \overline{\mathrm{DMS}} \right\rangle \quad (5)$$

The nighttime build up of DMS column concentration appears to be linear with time



ACPD
9, 16267–16294, 2009



(Fig. 6). The slope over these hours approximately represents the time rate of change in DMS column concentration, which includes the flux divergence plus any nocturnal chemical loss. At night, we assume [OH]=0 and $NO_3$ reaction is insignificant (this assumption is validated in the last section), so the loss term should be close to zero at night. From hour 01:00 to 10:00 UTC (or 20:00 to 05:00 local time), we calculate a surface DMS concentration increase of 2.6 $\mu$moles m$^{-2}$ day$^{-1}$. The mean nighttime surface flux obtained by eddy covariance was 3.2 $\mu$moles m$^{-2}$ day$^{-1}$, which means the nighttime entrainment flux needs to be 0.6 $\mu$moles m$^{-2}$ day$^{-1}$ to close the budget.

With a mean nighttime surface DMS concentration of 56 pptv and a decoupling parameter of 0.2, this entrainment flux corresponds to $\omega_e$=4 mm s$^{-1}$. While this $\omega_e$ only represents a nighttime value, it does agree very well with diurnal averages from previous studies in similar regions and seasons. Using a mixed-layer approach, Caldwell et al. (2005) found a 6-day average $\omega_e$ of 4±1 mm s$^{-1}$ during the East Pacific Investigation of Climate (EPIC) stratocumulus cruise in 2001. Combining satellite observations with National Centers for Environmental Prediction (NCEP) reanalysis, Wood and Bretherton (2004) determined an $\omega_e$ of 2∼6 mm s$^{-1}$ in the tropical and subtropical east Pacific, with a likely value of 4 mm s$^{-1}$ in the VOCALS region. Off the coast of California, where stratocumulus cloud-deck is also prevalent, direct measurements of $\omega_e$ from eddy covariance fluxes of three conserved scalars (DMS, ozone, and total water) immediately above and below the inversion led to a range of 1.2∼7.2 mm s$^{-1}$ (Faloona et al., 2005). At the limit of zero for the decoupling factor, the entrainment velocity calculated from Eq. (5) is lowered to 3 mm s$^{-1}$, still within the range of previous estimates.

### 2.5 Estimating effective OH

From the clear diurnal cycle and constant zonal flux to concentration ratio in the project averages, we observe no month-long trend in DMS. We can thus approximate DMS to be in a steady-state on that scale ($\partial\overline{[\mathrm{DMS}]}/\partial t$=0 when diurnally averaged).

For the purpose of this derivation we assume that the oxidation of DMS is solely due



ACPD
9, 16267–16294, 2009



to reactions with OH (Eqs. 1 and 2). The pseudo first-order rate constant $k_{PFO}$ in Eq. (5) can be expressed as $k_{OH}$, the total second order rate constant of the DMS-OH reaction ($k_{OH} = k_1 + k_2$), multiplied by [OH]. With an average MBL temperature of ~13°C during VOCALS-REx, we calculate $k_{OH}$ to be $7.9 \times 10^{-12}$ cm$^3$ molec$^{-1}$ s$^{-1}$, with the abstraction pathway accounting for 60% of the total oxidation.

Rearranging and expanding Eq. (5) leads to:

$$[OH] = \frac{F_0 - \omega_e(1-\alpha)[DMS_0]}{\left\langle \overline{DMS} \right\rangle k_{OH}} \quad (6)$$

Using an $\omega_e$ of 4 mm s$^{-1}$ and an $\alpha$ of 0.2, we find an effective OH concentration of $1.4 \times 10^6$ molec cm$^{-3}$ for VOCALS-REx, which is ~40% higher than the estimated global average, possibly due to high water content and solar radiation and relatively low anthropogenic influence in this region. An effective OH concentration of $1.4 \times 10^6$ molec cm$^{-3}$ implies a lifetime of 1.1 days for DMS with respect to OH in the MBL, well within the range of previous estimates of 0.5~2 days (e.g., Wine et al., 1981; Hynes et al., 1986). Allowing for a reasonable uncertainty of ±2 mm s$^{-1}$ in the entrainment velocity (due to diel variability, for example), the relative error in the calculated OH concentration is only ~12% (higher $\omega_e$, lower OH) because photochemical destruction was much greater than dilution due to entrainment. At a limit of $\alpha$=0 (i.e. no decoupling in DMS), OH is lowered to $1.2 \times 10^6$ molec cm$^{-3}$. The relative error in OH is roughly linearly related to the uncertainty in boundary layer height. An added benefit of estimating OH from the DMS flux and concentration is that both measurements are made by the same instrument, meaning that any calibration uncertainty in the instrument (such as flow rate or standard concentration) is negated, not affecting the final outcome.



ACPD
9, 16267–16294, 2009



## 3 Discussion

The above OH estimate is a diurnal average over a period of weeks. In reality, OH is only produced during the day when ozone can be photo-dissociated and is consumed completely when there is no light. The next logical step is to approximate the diel variability in OH, which has pronounced impacts on the evolution of sulfur species in the MBL, from DMS to $SO_2$ to sulfate.

### 3.1 Diel variability in OH

To approximate the diel profile of OH, we assume that the availability of light is the limiting factor in OH production since the reaction between $O(^1D)$ and water is rapid and water vapor is abundant. With CO being relatively constant away from the coast, the production of $O(^1D)$ from the photolysis of $O_3$ causes the diel variation in OH. Holland et al. (1998) found a correlation coefficient of 0.83 between OH concentration and the ozone photolysis frequencies. If this relationship holds, the concentration of OH can be approximated from the amount shortwave radiation at the surface. We first binned solar flux measured by the shipboard radiometer in the VOCALS region to the time-of-day, which expectedly led to a smooth curve with the peak insolation at ~17:00 UTC. Hourly hydroxyl concentrations ($[OH]_t$) were then made proportional to the magnitude of the solar flux, with the average equaling the OH-equivalent oxidant concentration of $1.4\times10^6$ molecules $cm^{-3}$. The radical peaked at about $5\times10^6$ molecules $cm^{-3}$ during the day and dropped to zero at night. While this method seems rather simplistic in comparison to photochemical models containing many photoactive species, the diel curve of OH agrees rather well with previous direct observations in the tropical/subtropical Pacific basin (e.g. Hofzumahaus et al., 1998; Davis et al., 2001; Mauldin et al., 2001).



ACPD
9, 16267–16294, 2009



### 3.2 Reproducing the diurnal cycle of DMS

The oxidation of DMS in the atmosphere has been modeled previously given an estimate of OH (Shon et al., 2001; Nowak et al., 2001). Using a similar approach and building upon Eq. (5), the surface DMS concentration at time $t$ can be written as:

$$\left\langle \overline{\mathrm{DMS}} \right\rangle_t = \left\langle \overline{\mathrm{DMS}} \right\rangle_{t-1} + F_{0,t-1} - \omega_e(1-\alpha)[\mathrm{DMS}_0]_{t-1} - k_{\mathrm{PFO},t-1} \left\langle \overline{\mathrm{DMS}} \right\rangle_{t-1} \quad (7)$$

For simplicity, we use the average $\omega_e$ of 4 mm s$^{-1}$, neglecting potential diel variation in the entrainment velocity as a result of infrared cooling. The implied DMS diurnal variation is not very sensitive to the choice of $\omega_e$ for the same reason as in Sect. 2.5.

We first equate, $k_{\mathrm{PFO},t}$, the pseudo first order reaction rate constant of DMS, simply to $k_{\mathrm{OH}}$ $[\mathrm{OH}]_t$, with $[\mathrm{OH}]_t$ being the radical concentration calculated from Sect. 3.1. Figure 7a shows the average observed surface DMS concentration in the VOCALS region, the approximated diel variability in OH, and DMS calculated from Eq. (7). It is clear that we can replicate the diurnal cycle of DMS fairly well. One might wonder whether the inclusion of other DMS oxidants can further improve the fit to observation. We will explore the importance of the nitrate radical in DMS oxidation next.

### 3.3 DMS oxidation by $NO_3$

Studies from Allan et al. (2000) in the relatively clean MBL at Mace Head suggested that the nocturnal level of the nitrate radical hovers on the order of a pptv, with reaction with DMS being its most important loss mechanism. Platt and Heintz (1994) estimated a globally averaged concentration of 3 pptv for $NO_3$. Not knowing how much $NO_3$ was present during VOCALS-REx, we apportion the total oxidative loss of DMS (determined from the equivalent-OH oxidant concentration) to fractions due to $NO_3$ and OH$\prime$ (the prime denotes the "actual" OH concentration). For example, if 10% of DMS oxidation was due to $NO_3$, the ratio between diurnal averaged $k_{\mathrm{NO_3}}$ $[\mathrm{NO_3}]$ and $k_{\mathrm{OH}}$ $[\mathrm{OH}]\prime$ should be 1:9. To mimic the diel variability in $NO_3$, we assume its nighttime level to be twice



ACPD
9, 16267–16294, 2009



the diurnal average and the daytime concentration to be zero. In actuality, $NO_3$ might not actually achieve steady state through out the night (Allan et al., 2000).

We found that the closest least-square fit (correlation coefficient greater than 0.9) is achieved between observed and calculated DMS when all of the DMS oxidation was due to OH, as any addition of $NO_3$ would degrade the fit. Schultz et al. (1999) showed that in the tropical South Pacific, the median $NO_x$ level was only 4 pptv in the lowest 2 km. In all likelihood, low levels of $NO_x$ and $O_3$ were limiting the production of $NO_3$ during VOCALS-REx.

Of course, our OH-equivalent oxidant concentration may still include reactions of DMS with $NO_3$ and halogen radicals. However, this effective concentration should only be slightly higher than the actual hydroxyl radical level because it appears that other oxidants were relatively unimportant.

## 4 Conclusions

We have demonstrated that a month-long average OH-equivalent oxidant concentration can be derived from the sea-to-air flux and concentration of DMS measured from a ship, using a simple mass balance method. To do so, we took advantage of the relatively well-understood chemistry of this sulfur gas and the simple dynamics in a stratocumulus-capped marine boundary layer. Judging from aircraft profiles during VOCALS-REx, the DMS concentration decreased linearly with altitude in the MBL as a result of boundary layer decoupling. On average, DMS immediately below the inversion was ~80% of the surface concentration.

MBL DMS concentration displayed the classic sinusoidal diurnal cycle, in which daily maxima and minima were found to be just after sunrise and just before sunset, respectively, as a result of the continuous build up through air-sea exchange and daytime consumption through photochemistry. From the nighttime build up of DMS column concentration, we estimated an entrainment velocity of 4 mm $s^{-1}$ by difference between the implied time-rate of change in column concentration and the observed surface flux.

The advective flux of DMS was found to be insignificant because the horizontal gradient in DMS was largely perpendicular to the mean wind direction. The calculated OH concentration of $1.4\times10^6$ molecules $cm^{-3}$ from the DMS budget equation agrees well with previous estimates, and represents a regional OH-equivalent oxidant concentration. Actual OH will be less by the extent that other DMS oxidants, such as nitrate- and halogen- radicals react with DMS. The OH estimate is relative insensitive to uncertainty in the entrainment velocity because the chemical loss term in the DMS budget equation is much larger than the entrainment flux term. A reasonable uncertainty of 2 mm $s^{-1}$ in $\omega_e$ leads to a difference of only ~12% in the derived effective OH concentration.

This equivalent OH concentration was fitted to the observed solar flux averaged to the time of day. We were able to use the resultant diel profile in OH, the mean observed DMS surface flux, and an entrainment velocity of 4 mm $s^{-1}$ to replicate the observed diurnal cycle of DMS in the MBL. The nitrate radical was also considered in the DMS oxidation, and was found to be unimportant during VOCALS-REx. The excellent agreement (correlation coefficient exceeding 0.9) between observed and calculated DMS suggests that our method of estimating equivalent OH is robust.

*Acknowledgement.* We thank the National Science Foundation for support of this work through grant ATM-0241611. Aircraft thermodynamic data was provided by NCAR/EOL under sponsorship of the NSF. Aircraft DMS data was provided by Drexel University. Special thanks to Chris W. Fairall, NOAA, Simon de Szoeke, Oregon State University, Rebecca M. Simpson, University of Hawaii, and the crew of the *R/V Ronald H. Brown.*

## References

Bandy, A. R., Thornton, D. C., Blomquist, B. W., Chen, S., Wade, T. P., Ianni, J. C., Mitchell, G. M., and Nadler, W.: Chemistry of dimethylsulfide in the equatorial Pacific atmosphere, Geophys. Res. Lett., 23(7), 741–744, 1996.

Bandy, A. R., Thornton, D. C., Tu, F. H., Blomquist, B. W., Nadler, W., Mitchell, G. M., and Lenchow, D. H.: Determination of the vertical flux of dimethylsulfide by eddy correlation and





atmospheric pressure ionization mass spectrometry (APIMS), J. Geophys. Res., 107(D24), 4743, doi:10.1029/2002JD002472, 2002.
Bates, T. S., Quinn, P. K., Covert, D. S., Coffman, D. J., Johnson, J. E., and Wiedensohler, A.: Aerosol physical properties and processes in the lower marine boundary layer: A comparison of shipboard sub-micron data from ACE-1 and ACE-2, Tellus, Ser. B, 52, 258–272, 2000.
Blomquist, B., Fairall, C. W., Huebert, B., Kieber D., and Westby, G.: DMS sea-air transfer velocity: Direct measurements by eddy covariance and parameterization based on the NOAA/COARE gas transfer model, Geophys. Res. Lett., 33(7), L07601, doi:10.1029/2006GL025735, 2006.
Bretherton, C. S. and Pincus, R.: Cloudiness and marine boundary layer dynamics in the ASTEX Lagrangian experiments. Part I: Synoptic setting and vertical structure, J. Atmos. Sci., 52, 2707–2723, 1995.
Bretherton, C. S., Uttal, T., Fairall, C. W., Yuter, S. E., Weller, R. A., Baumgardner, D., Comstock, K., Wood, R., and Rag, G. B.: The EPIC 2001 stratocumulus study, B. Am. Meteorol. Soc., 85(7), 967–977, 2004.
Caldwell, P., Bretherton, C. S., and Wood, R.: Mixed-Layer Budget Analysis of the Diurnal Cycle of Entrainment in Southeast Pacific Stratocumulus, J. Atmos. Sci., 62(10), 3775–3791, 2005.
Charlson, R. J., Lovelock, J. E., Andreae, M. O., and Warren, S. G.: Oceanic phytoplankton, atmospheric sulfur, cloud albedo and climate, Nature, 326, 655–661, 1987.
Chen, G., Davis, D. D., Kasibhatla, P., Bandy, A. R., Thornton, D. C., Huebert, B. J., Clarke, A. D., and Blomquist, B. W.: A study of DMS oxidation in the tropics: comparison of Christmas Island field observations of DMS, $SO_2$, and DMSO with model simulations, J. Atmos. Chem., 37, 137–160, 2000.
Davis, D., Grodzinsky, G., Chen, G., Crawford, J., Eisele, F., Mauldin, L., Tanner, D., Cantrell, C., Brune, W., Tan, D., Faloona, I., Ridley, B., Montzka, D., Walega, J., Grahek, F., Sandholm, S., Sachse, G., Vay, S., Anderson, B., Avery, M., Heikes, B., Snow, J., O'Sullivan, D., Shetter, R., Lefer, B., Blake, D., Blake, N., Carroll, M., and Wang, Y.: Marine latitude/altitude OH distributions: Comparison of Pacific Ocean observations with models, J. Geophys. Res.-Atmos., 106, 32691–32707, 2001.
Davis, D., Chen, G., Bandy, A., Thornton, D., Eisele, F., Mauldin, L. Tanner, D. Lenschow, D., Fuelberg, H., Huebert, B., Heath, J., Clarke, A., and Blake, D.: Dimethylsulfide oxidation in the equatorial Pacific: comparison of model simulations with field observations for DMS, $SO_2$, $H_2SO_4$(g), MSA(g), MS, and NSS, J. Geophys. Res., 104(D5), 5765–5784, 1999.



ACPD
9, 16267–16294, 2009



Donahue, N. and Prinn, R.: Nonmethane hydrocarbon chemistry in the remote marine boundary layer, J. Geophys. Res., 95, 18387–18411, 1990.
Edson, J. B., Hinton, A. A., Prada, K. E., Hare, J. E., and Fairall, C. W.: Direct covariance flux estimates from mobile platforms at sea, J. Atmos. Oceanic Technol., 15, 547–562, 1998.
Eisele, F. L. and Tanner, D. J.: Ion assisted tropospheric OH measurement, J. Geophys. Res., 96, 9295–9308, 1991.
Faloona, I., Lenschow, D., Campos, T., Stevens, B., van Zanten, M., Blomquist, B., Thornton, D., Bandy, A., and Gerber, H.: Observations of Entrainment in Eastern Pacific Marine Stratocumulus Using Three Conserved Scalars, J. Atmos. Sci., 62, 3268–3285, 2005.
Hard, T. M., O'Brien, R.J., Chan, C. Y., and Mehrabzadeh, A. A.: Tropospheric free radical determination by FAGE, Environ. Sci. Technol., 18, 768–777, 1984.
Hofzumahaus, A., Aschmutat, U., Brandenburger, U, Brauers, T., Dorn, H.-P., Hausmann, M., Heßling, M., Holland, F., Plass-Dülmer, C., and Ehhalt, D. H.: Intercomparison of tropospheric OH measurements by different laser techniques during the POPCORN campaign 1994, J. Atmos. Chem., 31, 227–246, 1998.
Holland, F., Aschmutat, U., Heßling, M., Hofzumahaus, A., and Ehhalt, D. H.: Highly time resolved measurements of OH during POPCORN using laser-induced fluorescence spectroscopy, J. Atmos. Chem., 31, 205–225, 1998.
Huebert, B. J., Blomquist, B. W., Hare, J. E., Fairall, C. W., Johnson, J. E., and Bates, T. S.: Measurement of the sea-air DMS flux and transfer velocity using eddy correlation, Geophys. Res. Lett., 31, L23113, doi:10.1029/2004GL021567, 2004.
Hynes, A. J., Wine, P. H., and Semmes, D. H.: Kinetics and mechanisms of OH reactions with organic sulfides, J. Phys. Chem., 90, 4148–4156, 1986.
Levy, H. I.: Normal Atmosphere: Large Radical and Formaldehyde Concentrations Predicted, Science, 173, 141–143, 1971.
Lilly, D. K.: Models of cloud-topped mixed layers under a strong inversion, Q. J. Roy. Meteor. Soc., 94, 292–309, 1968.
Lovelock, J. E., Maggs, R. J., and Rasmussen, R. A.: Atmospheric dimethyl sulphide and the natural sulphur cycle, Nature, 237(5356), 452–453, 1972.
Mauldin, R. L., Eisele, F. L., Cantrell, C. A., Kosciuch, E., Ridley, B. A., Lefer, B., Tanner, D. J., Nowak, J. B., Chen, G., Wang, L., and Davis, D.: Measurements of OH aboard the NASA P-3 during PEM-Tropics B, J. Geophys. Res., 106, 32657–32666, 2001.
Mount, G. H.: The measurement of tropospheric OH by long-path absorption, 1. Instrumenta-





tion, J. Geophys. Res., 97, 2427–2444, 1992.
Nowak, J. B., Davis, D. D., Chen, G., Eisele, F. L., Mauldin III, R. L., Tanner, D. J., Cantrell, C., Kosiuch, E., Bandy, A., Thorton, D., and Clarke, A.: Airborne observations of DMSO, DMS, and OH at marine tropical latitudes, Geophys. Res. Lett., 28(11), 2201–2204, 2001.
Platt, U. and Heintz, F.: Nitrate radicals in tropospheric chemistry, Isr. d. Chem., 34, 289–300, 1994.
Prinn, R., Cunnold, D., Simmonds, P., Alyea, F., Boldi, R., Crawford, A., Fraser, P., Gutzler, D., Hartley, D., Rosen, R., and Rasmussen, R.: Global Average Concentration and Trend for Hydroxyl Radicals Deduced From ALE/GAGE Trichloroethane (Methyl Chloroform) Data for 1978–1990, J. Geophys. Res., 97(D2), 2445–2461, 1992.
Prinn, R. G., Weiss, R. F., Miller, B. R., Huang, J., Alyea, F. N., Cunnold, D. M., Fraser, P. J., Hartley, D. E., and Simmonds, P. G.: Atmospheric trends and liftetime of $CH_3CCl_3$ and global OH concentrations, Science, 269, 187–192, 1995.
Russell, L. M., Lenschow, D. H., Laursen, K. K., Krummel, B., Siems, S. T., Bandy, A. R. Thornton, D. C., and Bates, T. S.: Bidirectional mixing in an ACE 1 marine boundary layer overlain by a second turbulent layer, J. Geophys. Res., 103, 16411–16432, 1998.
Sander, S. P., Golden, D. M., Kurylo, M. J., Moortgat, G. K., Wine, P. H., Ravishankara, A. R., Kolb, C. E., Molina, M. J., Finlayson-Pitts, B. J., Huie, R. E., and Orkin, V. L.: Chemical Kinetics and Photochemical Data for Use in Atmospheric Studies, Evaluation Number 15, Jet Propulsion Laboratory, Pasadena, CA (available at http://jpldataeval.jpl.nasa.gov/), 2006.
Seinfeld, J. H. and Pandis, S. N.: Atmospheric chemistry and physics: from air pollution to climate change 2nd ed. Wiley-Interscience, Hoboken, New Jersey, USA, 2006.
Shon, Z. H, Davis, D., Chen, G., Grodzinsky, G., Bandy, A., Thornton, D., Sandholm, S., Bradshaw, J., Stickel, R., Kok, G., Mauldin, L., Tanner D., and Eisele, F.: Evaluation of the DMS Flux and its Conversion in $SO_2$ Over the Southern Ocean, Atmos. Environ., 35, 159–172, 2001.
Shultz M. G., Jacob, D. J., Wang, Y., Logan, J. A., Atlas, E. L., Blake, D. R., Blake, N. J., Bradshaw, J. D., Fenn, M. A., Flocke, F., Gregory, G. L., Heikes, B. G., Sachse, G. W., Sandholm, S. T., Shetter, R. E., Singh, H. B., Talbot, R. W.: On the origin of tropospheric ozone and $NO_x$ over the tropical South Pacific, J. Geophys. Res., 104, 5829–5843, 1999.
Spivakowsky, C. M., Logan, A. J., Montzka, S. A., Balkanski, Y. J., Foreman-Fowler, M., Jones, D. B. A., Horowitz, L. W., Fusco, A. C., Brenninkmeijer, C. A. M., Prather, M. J., Wofsy, S. C., and McElroy, M. B.: Three dimensional climatological distribution of tropospheric OH:

Update and evaluation, J. Geophys. Res., 105, 8931–8980, 2000.

Stevens, B., Lenschow, D. H., Vali, G., Gerber, H., Bandy, A., Blomquist, B., Brenguier, J. L., Bretherton, C. S., Burnet, F., Campos, T., Chai, S., Faloona, I., Friesen, D., Haimov, S., Laursen, K., Lilly, D. K., Loehrer, S. M., Malinowski, S. P., Morley, B., Petters, M. D., Rogers, D. C., Russell, L., Savic-Jovcic, V., Snider, J. R., Straub, D., Szumowski, M. J., Takagi, H., Thornton, D. C., Tschudi, M., Twohy, C., Wetzel, M., and van Zanten, M. C.: Dynamics and Chemistry of Marine Stratocumulus – DYCOMS-II, 2003: B. Am. Meteorol. Soc., 84, 579–593, 2003.

Stickel R. E., Zhao, Z., and Wine, P. H.: Branching ratios for hydrogen transfer in the reactions of OD radicals with $CH_3SCH_3$ and $CH_3SC_2H_5$, Chem. Phys. Lett., 212, 312–318, 1993.

Wallington, T. J., Ellermann, T., and Nielsen, O. J.: Atmospheric chemistry of dimethylsulfide: UV spectra and self-reaction kinetics of $CH_3SCH_2$ and $CH_3SCH_2O_2$ radicals and kinetics of the reactions $CH_3SCH_2 + O_2$ $CH_3SCH_2O_2$ and $CH_3CH_2O_2 + NO \rightarrow CH_3SCH_2O_2 + NO_2$, J. Phys. Chem., 97, 8442–8449, 1993.

Wine, P. H., Kreutter, N. M., Gump, C. A., Ravishankara, A. R.: Kinetics of OH reactions with the atmospheric sulfur compounds $H_2S$, $CH_3SH$, $CH_3SCH_3$, $CH_3SSCH_3$, J. Phys. Chem., 85, 2660–2665, 1981.

Wood, R. and Bretherton, C. S.: Boundary Layer Depth, Entrainment, and Decoupling in the Cloud-Capped Subtropical and Tropical Marine Boundary Layer, J. Climate, 17, 3576–3588, 2004.

Yvon, S. A., Plane, J. M. C., Nien, C.-F., Cooper, D. J. and Saltzman, E. S.: The interaction between the nitrogen and sulfur cycles in the marine boundary layer, J. Geophys. Res., 101, 1379–1386, 1996.





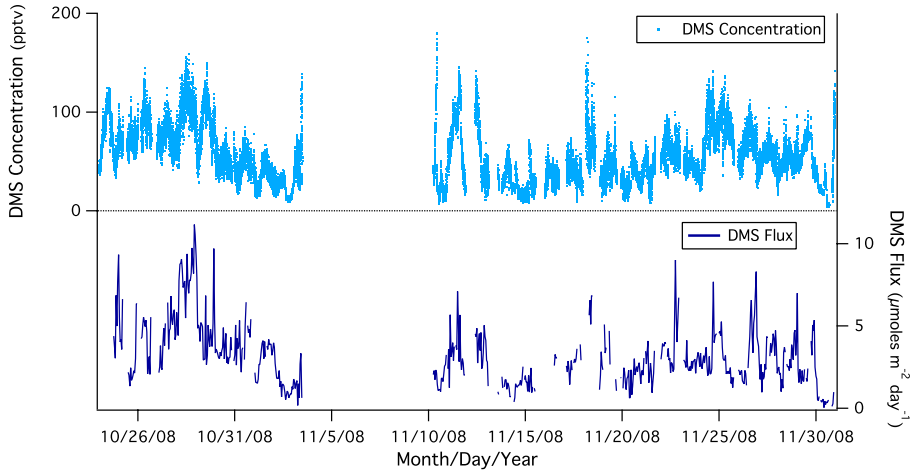


**Fig. 1.** DMS concentration (top) and surface flux (bottom) from the *RHB* during VOCALS-REX. Incidents of elevated atmospheric DMS concentration and flux usually corresponded to spikes in $DMS_w$ on the edges of localized eddies.



ACPD
9, 16267–16294, 2009



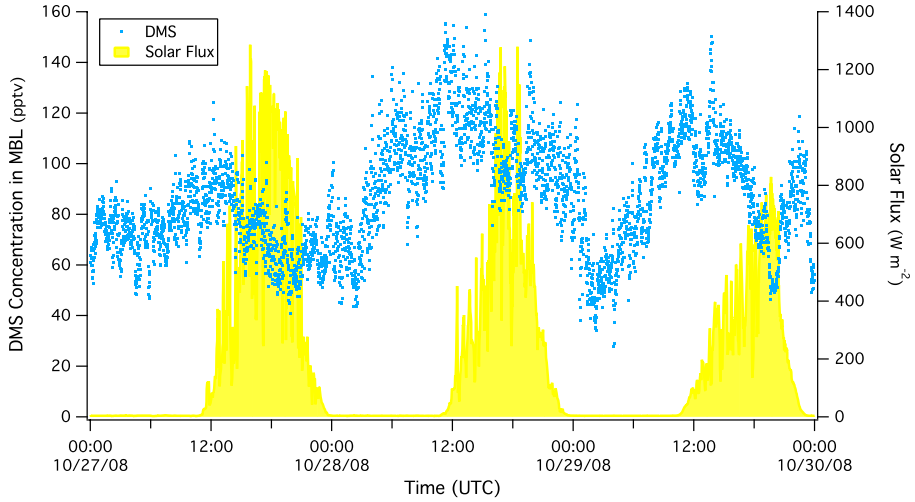


**Fig. 2.** Examples of diurnal cycle in DMS observed during VOCALS-REX on board of the *RHB*, along with solar flux measured from a shipboard radiometer. The maxima and minima in DMS were usually observed just after sunrise and just before sunset, respectively.



ACPD
9, 16267–16294, 2009

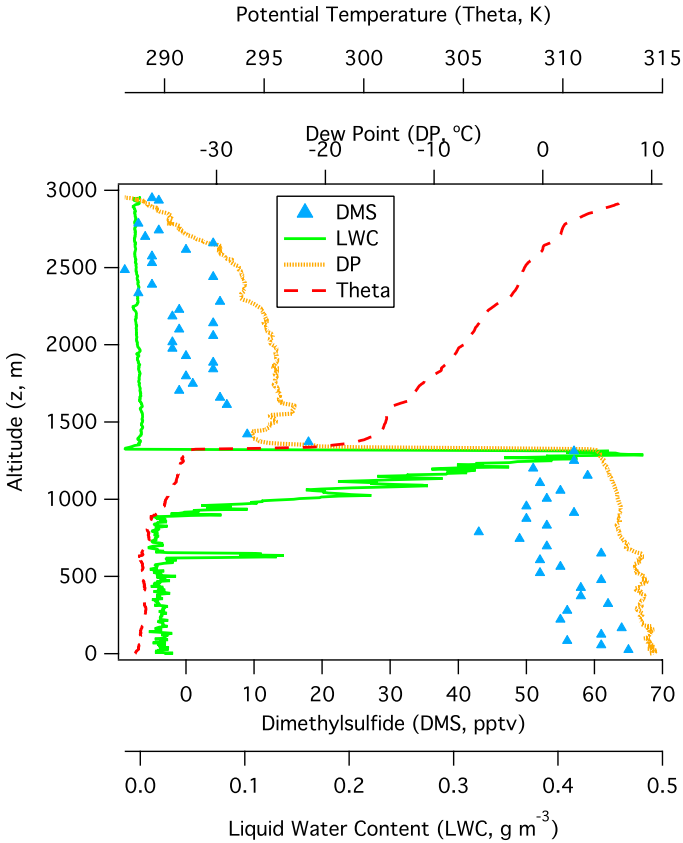


**Fig. 3.** A typical profile of the lower troposphere determined from the C-130 (12:24~12:35 UTC on 25 October during Research Flight No. 5). DMS decreased gradually with altitude in the MBL (the lower ~1300 m in this case) and dropped to zero in the FT. A strong inversion atop the stratocumulus cloud deck (indicated by high liquid water content) was defined by sharp gradients in dew point and potential temperature.



ACPD
9, 16267–16294, 2009



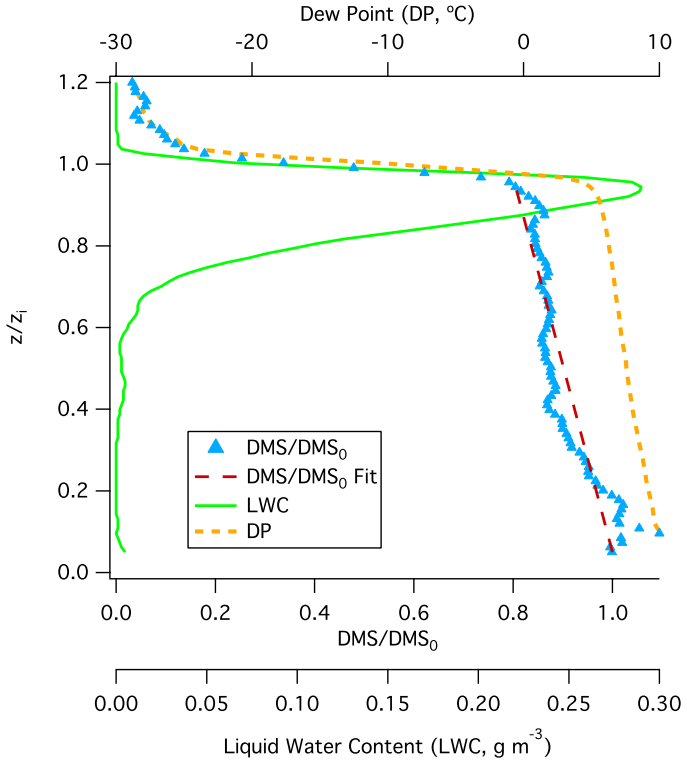


**Fig. 4.** Averaged profile from the C-130: liquid water content, potential temperature, dew point, and [DMS] normalized to its surface value. Altitude was normalized to the inversion height. DMS at height is related to DMS at the surface by the linear regression fit $1-\alpha(z/z_i)$, with $\alpha$ being the DMS "decoupling" parameter and determined to be 0.2 on average for VOCALS.



ACPD
9, 16267–16294, 2009





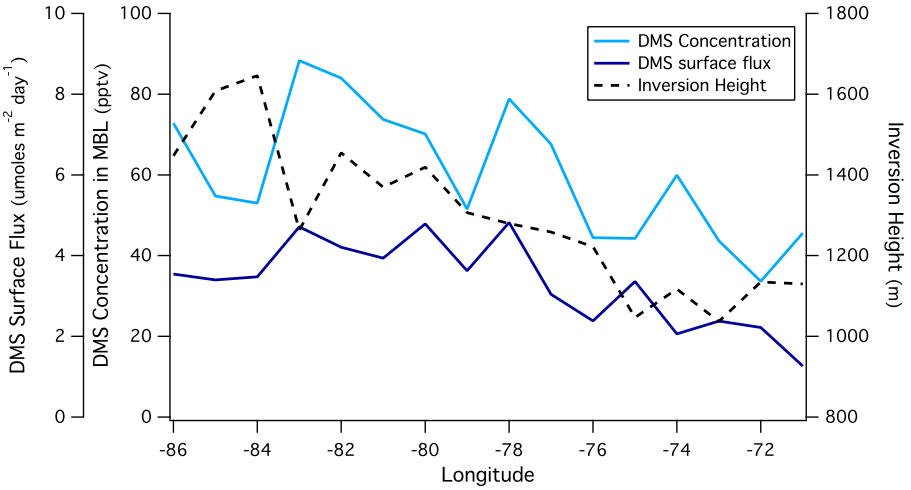


**Fig. 5.** Zonal average of atmospheric DMS concentration and surface flux from the *RHB* along 20±2° S, as well as the inversion height determined from C-130 flight profiles. The ratio between DMS flux to concentration was largely constant, while the boundary layer was deeper offshore.



ACPD
9, 16267–16294, 2009



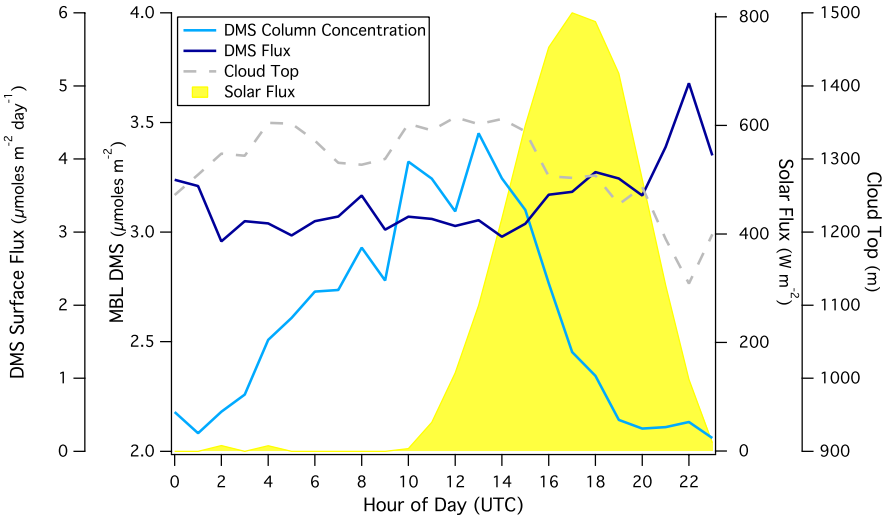


**Fig. 6.** DMS surface flux, concentration, and shortwave radiation measured from the *RHB* in the VOCALS region averaged to the time of day. DMS concentration shows the classic sinusoidal diurnal cycle due to continuous build up via air-sea exchange and daytime OH oxidation. The cloud top was generally higher at night than during the day.



ACPD
9, 16267–16294, 2009





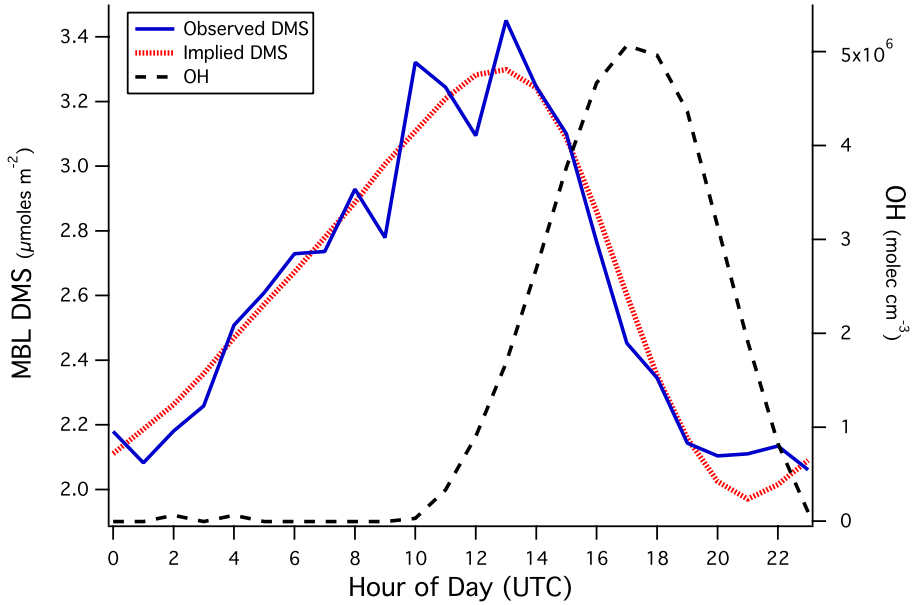


**Fig. 7.** Observed and implied DMS diurnal cycle, as well as OH profile estimated from solar flux. DMS was calculated from observed surface concentration and flux, approximated effective OH diurnal profile, with an entrainment rate of 4 mm $s^{-1}$. To investigate the importance of the nitrate radical, OH-equivalent oxidant concentration was apportioned to OH and $NO_3$. Even 1% of oxidation of DMS by $NO_3$ leads to a lower correlation coefficient between the implied and observed DMS. That no $NO_3$ is required by the fit supports our early assumption that nocturnal oxidation is negligible.



ACPD
9, 16267–16294, 2009